Aerosol choices influence precipitation changes across future scenarios

Isabel L. McCoy[1,2], Mika Vogt[3], and Robert Wood[3]

[1]Rosenstiel School of Marine and Atmospheric Science, University of Miami, Miami, FL, 33149-1031, USA
[2]University Corporation for Atmospheric Research, Boulder, CO, 80307-3000, USA
[3]Department of Atmospheric Sciences, University of Washington, Seattle, WA, 98195-1640, USA

Key Points:

- Atmospheric energy budgets are used to constrain absorbing aerosol influences on 21st century precipitation in ScenarioMIP projections.
- Shared socioeconomic pathways with aerosol cleanup policies can significantly augment 21st century global precipitation.
- Impacts of regional aerosol changes on precipitation are equal or larger than the influence from atmospheric circulation changes.

Corresponding author: Isabel L. McCoy, imccoy@ucar.edu

Abstract

Future precipitation changes are controlled by the atmospheric energy budget, with radiative changes driven by temperature, water vapor, and absorbing aerosol playing dominant roles. Atmospheric energy budgets are calculated for different Shared Socioeconomic Pathways (SSPs) using ScenarioMIP projections from phase 6 of the Climate Model Intercomparison Project and are used to quantify the influence of 21st century aerosol cleanup on precipitation. Absorbing aerosol influences on shortwave absorption are isolated from the effects of water vapor. Apparent hydrologic sensitivity is ∼40% higher for the *Middle of the Road* (SSP2-4.5) scenario with aerosol cleanup than for the *Regional Rivalry* (SSP3-7.0) scenario that maintains aerosol. Regionally, cleanup-induced changes in the atmospheric energy budget are of a similar magnitude to the precipitation increases themselves and are larger than the influence of changes in atmospheric circulation. Policy choices about future absorbing aerosol emissions will therefore have major impacts on global and regional precipitation changes.

Plain Language Summary

Precipitation changes will have a temperature-dependent and a temperature-independent part of their response to climate change. Water vapor contributes primarily to the former while well-mixed greenhouse gases will influence both. The temperature-independent response will be impacted by absorbing aerosol emissions. This is examined through an atmospheric energy budget where precipitation (i.e., latent heat) balances other energy sources and sinks in the atmosphere (i.e., sensible heat, shortwave and longwave radiation). We utilize a novel set of global climate model simulations that incorporate varied socioeconomic choices over the 21st century to study real-world implications of future aerosol policies on precipitation. Reductions in absorbing aerosol amount help precipitation to increase because less shortwave absorption will occur in the atmosphere and, on average, other energy contributions do not change per degree warming. Global precipitation change per degree of global warming is ∼40% higher for socioeconomic pathways where aerosol cleanup occurs. Regional precipitation changes associated with regional aerosol changes are larger than those associated with changes in atmospheric circulation. Policy choices for aerosol emissions will thus have a critical impact on the future availability of water, both globally and regionally.

1 Introduction

Regional and global changes in precipitation are expected over the 21st century driven by increasing greenhouse gases, changes in aerosols, and changes in land use (Allan et al., 2020). These factors influence precipitation by changing atmospheric longwave emission and shortwave absorption (Pendergrass & Hartmann, 2014). A major fraction of the inter-model variance in global mean precipitation increase has been shown to be associated with uncertainties in clear sky shortwave absorption (Pendergrass & Hartmann, 2012; DeAngelis et al., 2015), changes in which are controlled primarily by water vapor path (WVP) and absorbing aerosols.

Emissions of aerosols over the 21st century are expected to change markedly, with changes strongly dependent upon socioeconomic pathways (Lund et al., 2019). WVP increases with global mean temperature, closely following Clausius-Clapeyron (C-C) scaling of ∼7% K^{-1} (Held & Soden, 2006; Allan et al., 2014). Precipitation increases much more slowly with temperature (Held & Soden, 2006) and is constrained by the atmospheric energy budget (Pendergrass & Hartmann, 2014).

Precipitation changes can be separated into temperature-dependent and temperature-independent responses (Allen & Ingram, 2002; Andrews et al., 2010). Absorbing aerosols influence precipitation through the latter. WVP contributes primarily to the former as

it is strongly tied to temperature. Although WMGHGs primarily drive the temperature-dependent response, they also contribute to the fast precipitation response (Richardson et al., 2018). In order to reduce uncertainties in projected precipitation, it is important to understand the role that aerosols play in the fast response and assess the impact of different aerosol policy choices on precipitation.

In the most recent Coupled Model Intercomparison Project (CMIP6), models ran scenarios designated by Shared Socioeconomic Pathways (SSPs) — representing possible policies over the next century — and 2100 forcing levels in W m^{-2} (Eyring et al., 2016). Different policies strongly influence absorbing aerosol changes, impacting future precipitation through the temperature-independent response. These ScenarioMIP simulations (described in Section 2) allow an examination of how policy decisions can influence different aspects of future climate.

We use an atmospheric energy budget framework to estimate contributions from projected changes in absorbing aerosols to changes in global and regional precipitation. We focus especially on two scenarios, SSP2-4.5 and SSP3-7.0, as they offer a contrasting aerosol strategy (clean up vs. no clean up, respectively) at intermediate radiative forcing pathways. Section 2 describes the models and methods. Global and regional precipitation change results are presented in Sections 3 and 4, respectively. Section 5 presents a comparison of different methods to constrain the contribution of changes in absorbing aerosols to the precipitation response across scenarios.

2 Materials and Methods

2.1 CMIP6 ScenarioMIP Simulations

We examine climate model projections from four Tier-1 ScenarioMIP scenarios from CMIP6. Each scenario has a distinct SSP and a different level of forcing following the Representative Concentration Pathways (RCPs) used in previous CMIPs (Neill et al., 2016; Riahi et al., 2017). The SSPs factor in differences in societal development related to societal concerns around climate change. Lower SSPs (e.g., SSP1: *Sustainability*, SSP2: *Middle of the Road*) have fewer challenges to climate mitigation and adaptation while higher SSPs have more (e.g., SSP3: *Regional Rivalry*, SSP5: *Fossil-fueled Development*) (Riahi et al., 2017).

SSP1-2.6 uses the RCP2.6 pathway, is the most weakly-forced scenario considered (experiencing less than 2°C warming by 2100 in the multi-model mean), and undergoes substantial land-use change. SSP2-4.5 undergoes intermediate forcing, is an update to RCP4.5, and has less extreme changes in aerosol and land use compared to other SSPs. SSP3-7.0 has a higher forcing (an update to RCP7.0). In particular, it has large land use changes and maintains high emissions of short lived climate forcers (e.g., aerosols) until 2100. Finally, SSP5-8.5 is the most strongly-forced scenario considered, an update to RCP8.5.

Our analysis focuses on changes between the present day (2015-2025) and the end of this century (2090-2100) using composites from 19 CMIP6 models (Table S1). All currently available models with outputs necessary for estimating absorbing aerosol contributions to the atmospheric energy budget are included, with absorbing aerosol optical depth at 550nm wavelength ($AAOD$) used to describe absorbing aerosol amount. Global changes in key quantities for the four scenarios are listed in Table S2 while trends in CO_2 and WVP and their correspondence are shown in Fig. S1. The 21st century trend in $AAOD$, which is primarily driven by changes in black carbon emissions, varies strongly across the four scenarios (Fig. 1a). Strong $AAOD$ reductions in SSP1-2.6, SSP2-4.5 reflect aggressive aerosol cleanup policies, weaker reductions occur in SSP5-8.5, and SSP3-7.0 is distinguished by having no $AAOD$ reductions over this period (Turnock et al., 2020).

2.2 Absorbing aerosol impacts on the atmospheric energy budget

To quantify the impact of absorbing aerosol changes on precipitation, we adopt an atmospheric energy budget approach (e.g., Pendergrass and Hartmann (2014)). Globally, precipitation change (ΔP) reflects change in atmospheric latent heating (ΔLH), which, together with atmospheric sensible heating (ΔSH), must be balanced by reductions in absorbed energy in the net atmospheric longwave (ΔLW) and shortwave (ΔSW):

$$-L_v \Delta P = -\Delta LH = \Delta SH + \Delta SW + \Delta LW \quad (1)$$

where L_v is the latent heat of vaporization. Water vapor and absorbing aerosol changes dominate ΔSW (Richardson et al., 2018). We use a multiple regression to separate these contributions. For each scenario, global annual multi-model mean time series of WVP, $AAOD$ and net SW are constructed. The resulting fit, parabolic in ΔWVP and linear in $\Delta AAOD$, explains 99.8% of the variance of ΔSW at 95% confidence (Fig. S2):

$$\Delta SW = a \cdot \Delta WVP + b \cdot (\Delta WVP)^2 + c \cdot \Delta AAOD \quad (2)$$

where a=0.694±0.005 W kg^{-1}, b=-0.016±0.001 W kg^{-2} m^2, and c=493±4 W m^{-2}, with errors providing 95% confidence intervals. We note that c is within the standard deviation of the multi-model mean CMIP5 AeroCom coefficient value, 525±165 W m^{-2} (see Table 3 in Myhre et al., 2013). The quadratic term in ΔWVP is needed to account for the sub-linear dependency of solar absorption on WVP (Lacis & Hansen, 1974) but is relatively weak, contributing only 5-15% of the overall ΔWVP contribution to SW absorption.

3 Changes in Global Precipitation over the 21st century

Within each scenario (i.e., for fixed radiative forcing), global mean precipitation ΔP increases at ∼2.5% per degree of global mean warming (Fig. 1b) consistent with 2-3% K^{-1} in earlier studies (Samset et al., 2018). Although this slope (i.e., the hydrologic sensitivity, η), is consistent across SSPs (Table S2), the intercepts of the ensemble member fits differ significantly. The SSP differences in response can also be described by the apparent hydrologic sensitivity, $\eta_a = L_v \Delta P / \Delta T$ (Allan et al., 2020), using the multi-model means (Table S2). SSP3-7.0 stands out as it has a substantially lower ΔP than would be expected from the ΔT experienced in this scenario. Indeed, instead of falling between SSP2-4.5 and SSP5-8.5, the SSP3-7.0 line nearly overlaps the SSP5-8.5 line (Fig. 1b).

To explore this further, Fig. 1c shows multi-model mean changes in the atmospheric budget terms for the four scenarios. As ΔT increases, all terms correspondingly increase in magnitude. Negative ΔLW indicates increasing atmospheric radiative cooling as temperature increases (Pendergrass & Hartmann, 2014), which is remarkably linear in ΔT. In contrast, changes in ΔSW, ΔSH, and ΔLH ($\equiv L_v \Delta P$) all show deviations from linear behavior. In particular, SSP3-7.0 has a markedly stronger increase in ΔSW and, as a result, a muted increase in ΔLH and thus precipitation. The lack of deviation by ΔLW in SSP3-7.0 suggests that anomalies in WMGHGs and WVP are unlikely to be driving the anomalous precipitation response in SSP3-7.0. Instead, ΔSW is likely a major driver of the unusual behavior seen in SSP3-7.0 ΔP (Fig. 1b, c). The lack of aerosol cleanup in this scenario (Fig. 1a) may be muting precipitation increases over the 21st century compared with scenarios that undergo cleanup.

We examine two scenarios in detail, SSP2-4.5 and SSP3-7.0, that represent intermediate RCP pathways in the ScenarioMIP simulations but with substantially different SSP aerosol emission choices. Using Eq. 2, we quantify the contributions of $\Delta AAOD$ (ΔSW_{AAOD}) and ΔWVP (ΔSW_{WVP}) to ΔSW. These are shown along with the remaining energy budget terms from Eq. 1 in Fig. 2. To control for differences in forcing (i.e., temperature change) between scenarios, energy budgets are examined per degree of global warming and terms are reported as sensitivities. The normalized precipitation change (i.e.,

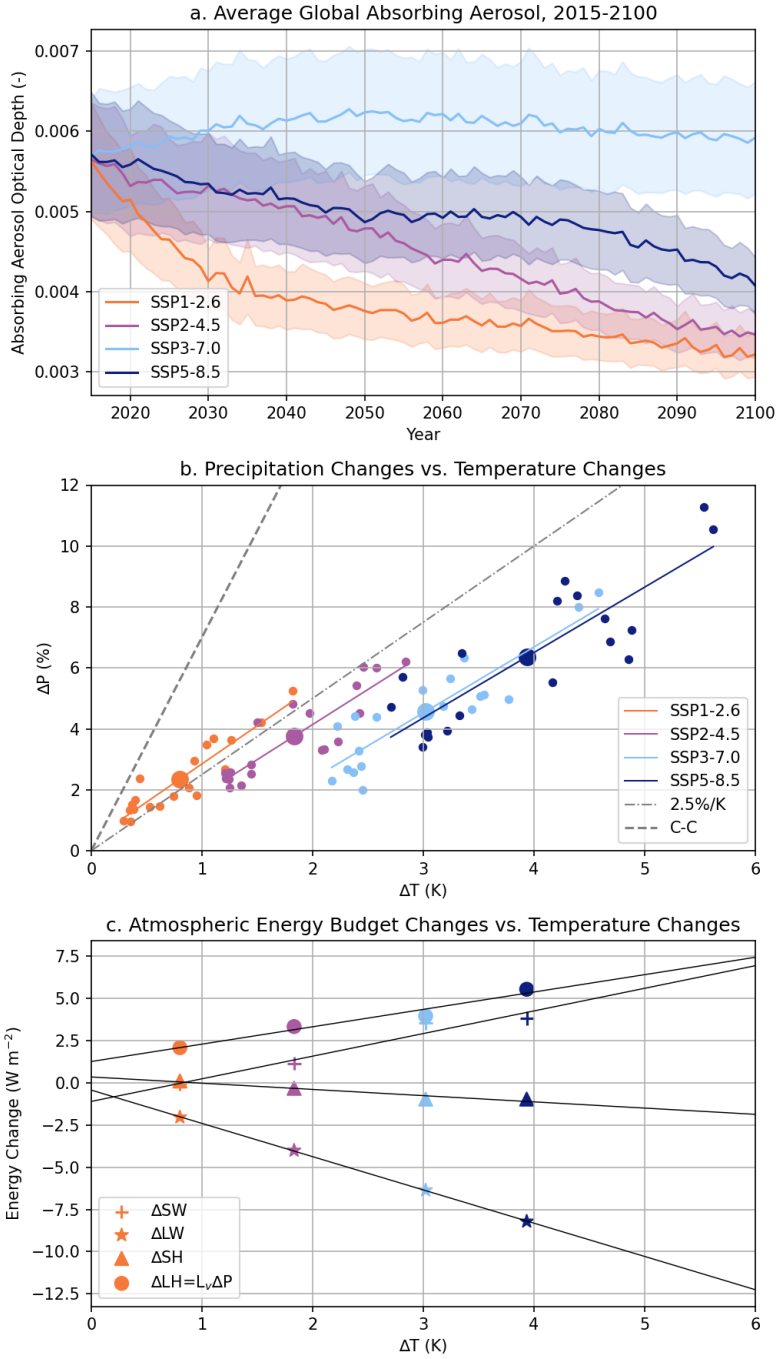

Figure 1. (a) Global multi-model ensemble mean (line) and corresponding standard error (shading) for $AAOD$ by scenario across period of interest (2015-2100). Global mean changes in (b) precipitation and (c) atmospheric energy budget terms plotted as a function of global mean surface air temperature changes. Changes are computed as the difference between two ten-year periods, 2090-2100 and 2015-2025. In (b), projections from each contributing model (small circles) and the scenario multi-model mean (large circles) are shown. The ratio of the ensemble mean $\Delta P/\Delta T$ represents the apparent hydrologic sensitivity. The slope of the best fit line through the individual ensemble members for each scenario represents the hydrologic sensitivity (Table S2), which is ~2.5%/K for each scenario (dot-dash). The C-C response (i.e., ~7%/K) is included for reference (dash).

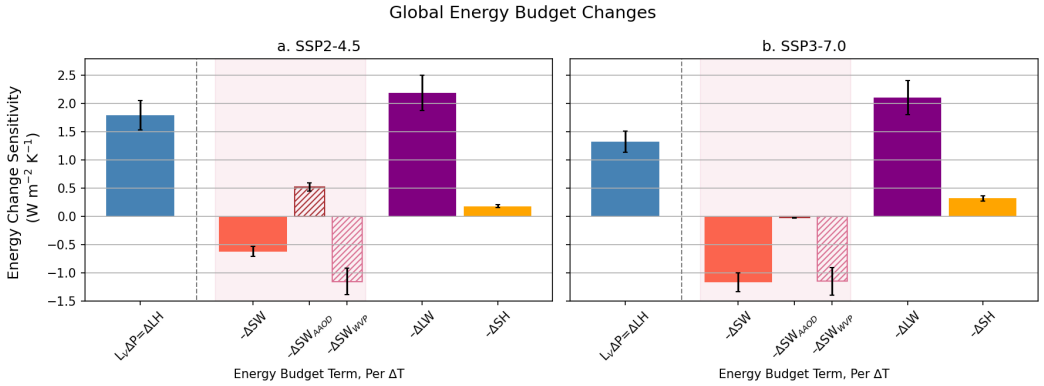

Figure 2. Global changes in the atmospheric energy budget (2015-2025 to 2090-2100) for two scenarios with contrasting aerosol choices: (a) SSP2-4.5 and (b) SSP3-7.0. Energy budget terms are normalized by the change in global mean surface air temperature and expressed as sensitivities. ΔSW (solid) is decomposed into two (hatched) components, ΔSW_{AAOD} and ΔSW_{WVP}, based on Eq. 2. Solid bars on the right of the dashed line sum to the precipitation change on the left following Eq. 1. Bars represent multi-model means while error bars represent two standard errors based on the variability in the multi-model mean 10-year periods propagated through the change and normalization calculations. Standard errors for ΔSW components also include coefficient uncertainties.

apparent hydrologic sensitivity) is 40% larger for SSP2-4.5 than for SSP3-7.0. ΔLW and ΔSW_{WVP} sensitivities are remarkably similar between these scenarios, indicating they are not the primary drivers of differences in η_a. Instead, the majority of the difference in η_a can be explained by differences in absorbing aerosol pathways in the two scenarios, with a much smaller contribution from ΔSH. Aerosol cleanup in SSP2-4.5 reduces SW absorption, offsetting approximately 40% of the increased SW absorption driven by increased WVP (Fig 2a). This results in larger global precipitation increases in SSP2-4.5 while the lack of cleanup in SSP3-7.0 results in muted 21st century precipitation increases (Fig 2b).

4 Factors Influencing Regional Precipitation Changes

Given that aerosol cleanup choices can significantly effect global precipitation changes, we now explore the extent to which regional $\Delta AAOD$ is expected to influence regional precipitation over the 21st century. Geographic patterns of $\Delta AAOD$ are highly heterogeneous. We focus on two regions with striking 21st century $\Delta AAOD$ (Table S3, Fig. S3), which are also thought to be dominated by the temperature-independent precipitation response (Samset et al., 2016): equatorial Africa (15°S-15°N, 30°W-30°E) and southeastern Asia (0-45°N, 60-130°E). Strong aerosol cleanup occurs in both regions in SSP2-4.5 while in SSP3-7.0 aerosol loadings increase in Equatorial Africa and show little overall change in SE Asia.

The regions studied here are sufficiently large (>3000 km in scale) that atmospheric energy and water budgets are useful for assessment of their precipitation changes (Dagan et al., 2019a; Dagan & Stier, 2020). On a regional scale the energy and moisture budgets are:

$$L_v \Delta P = -\Delta SH - \Delta SW - \Delta LW + \Delta div(s) \tag{3}$$

$$\Delta P = \Delta E - \Delta div(q_v) = \Delta LH / L_v - \Delta div(q_v) \tag{4}$$

where $div(s)$ and $div(q_v)$ are divergences of dry static energy and column integrated moisture, respectively, reflecting the exports of energy and moisture required to balance the regional budgets.

Fig. 3 presents contributions of each of the normalized terms in Eqns. 3 and 4 to the overall, normalized ΔP experienced in each region under SSP2-4.5 and SSP3-7.0. Examining the simpler water budget (Eq. 4) first, we find ΔLH sensitivity differs between SSPs but not regionally: SSP2-4.5 has a larger change than SSP3-7.0. However, $\Delta div(q_v)$ sensitivity varies more between regions than by SSP: SE Asia experiences increased moisture convergence while Equatorial Africa experiences the opposite. The net result is a substantial variation between both region and scenario for regional η_a.

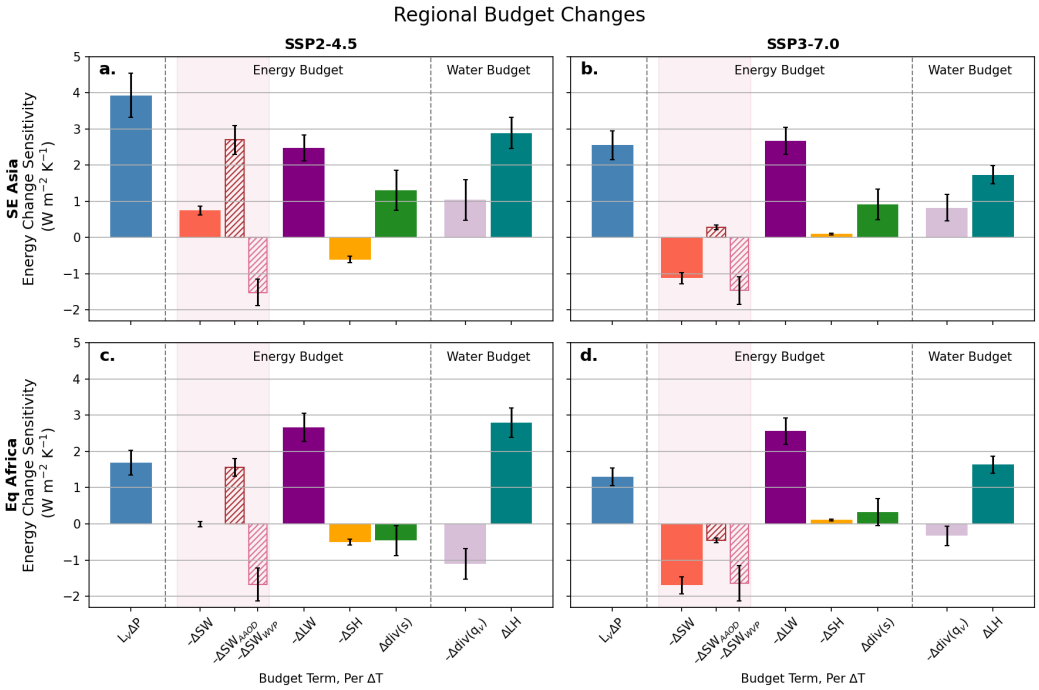

Figure 3. Regional atmospheric energy and moisture budget changes (2015-2025 to 2090-2100) for SSP2-4.5 (panels a, c) and SSP3-7.0 (panels b, d) for Southeast Asia (0-45°N, 60-130°E; panels a, b) and Equatorial Africa (15°S-15°N, 30°W-30°E; panels c, d). Budget term normalization, ΔSW decomposition, bar and error bar meanings as in Fig. 2. Normalized energy budget terms (solid bars between dashed lines) sum to the normalized precipitation change (left) following Eq. 3 while normalized water budget terms (solid bars to the right of dashed lines) sum following Eq. 4.

The regional energy budget provides insight into variability in regional η_a (Fig. 3). As in the global budget (Fig. 2), ΔLW and ΔSW_{WVP} variation across region and SSP is very small, implying that factors other than the atmospheric radiative effects of WMGHGs and WVP are controlling regional and inter-scenario differences in precipitation response. Instead, ΔSW_{AAOD}, ΔSH, and $\Delta div(s)$ differences control variability in regional η_a. Absorbing aerosol changes (ΔSW_{AAOD}) are the leading contributor to energy budget changes between the two scenarios, in both regions (left versus right panels, Fig. 2), implying that a substantial fraction of the markedly higher regional η_a for SSP2-4.5 can be explained by aerosol cleanup policies. This is also the case in Equatorial Africa, where cleanup in SSP2-4.5 occurs but aerosol loadings actually increase in SSP3-7.0. Increased

AAOD in the tropics may influence precipitation through thermally driven circulation changes from modification of $div(s)$ (Dagan et al., 2019b, 2021) but absorbing aerosol perturbations over Eq. Africa and SE Asia are expected to have a small effect (Dagan et al., 2021). Indeed, changes in both $\Delta div(s)$ and $\Delta div(q_v)$ sensitivity between scenarios are considerably smaller than those in ΔSW_{AAOD}. This implies that regional precipitation changes between scenarios are more strongly controlled by aerosol absorption changes than they are by changes in the import or export of energy and moisture, suggestive of a relatively small role for atmospheric circulation changes.

To better understand the circulation responses, we estimate the thermodynamic contribution to precipitation-evaporation ($P-E$) changes that would occur in the absence of changes in the lower tropospheric circulation. Using Eq. 5, we estimate the moisture convergence $\Delta div(q_v)_{thermo}$ driven solely by increased WVP (Fig. 4) assuming the circulation remains fixed (i.e., Held and Soden (2006)):

$$\Delta(P-E) \approx \alpha(P-E)\Delta T = -\Delta div(q_v)_{thermo} \tag{5}$$

where $\alpha \approx 0.07$. We use $\Delta div(q_v)_{thermo}$ in Eq. 4 to estimate a predicted change in precipitation, ΔP_{thermo}, absent circulation changes. The difference, $\Delta P_{circ} = \Delta P - \Delta P_{thermo}$, is an estimate of the influence that circulation has on regional precipitation. Similarly, the difference $\Delta div(q_v)_{circ} = \Delta div(q_v) - \Delta div(q_v)_{thermo}$ is an estimate of the circulation influence on regional moisture convergence changes.

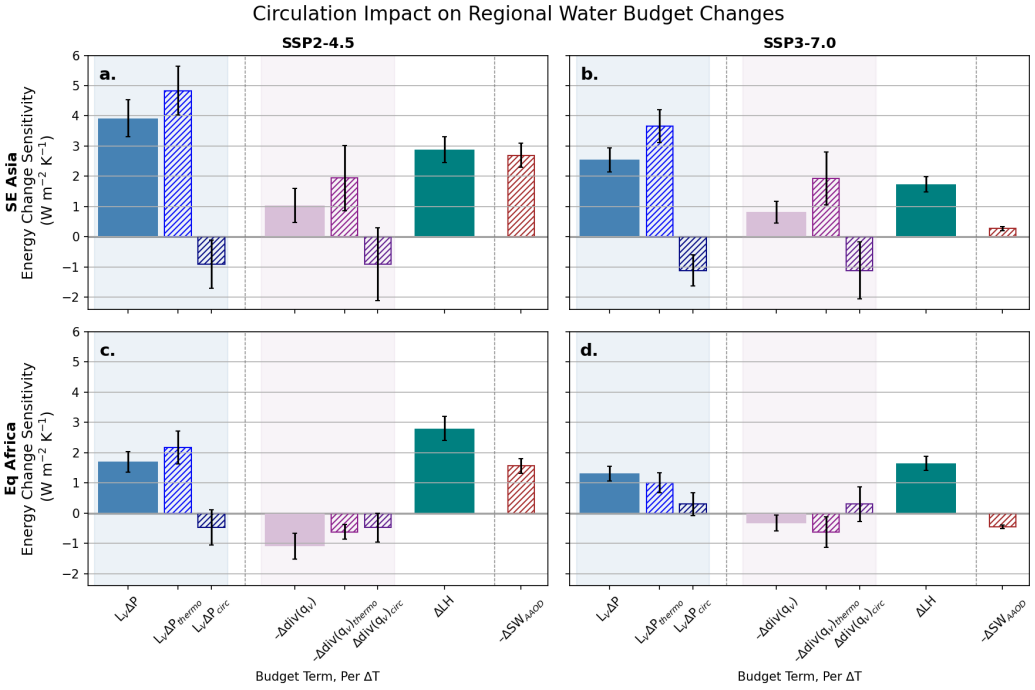

Figure 4. Estimation of regional changes in circulation (2015-2025 to 2090-2100) for SSP2-4.5 (a, c) and SSP3-7.0 (b, d) for Southeast Asia (a, b) and Equatorial Africa (c, d). Budget term normalization, bar and error bar meanings as in Fig. 3. Thermodynamic ($\Delta div(q_v)_{thermo}$, ΔP_{thermo}) and circulation ($\Delta div(q_v)_{circ}$, ΔP_{circ}) contributions to the total ($\Delta div(q_v)$, ΔP) are estimated using Eqns. 5 and 4. ΔSW_{AAOD} (Fig. 3), the only ΔSW component changing between regions and SSPs, is included for reference.

Comparing the magnitude of the circulation change influence on precipitation (ΔP_{circ}) to the magnitude of the AAOD influence on SW (ΔSW_{AAOD}), we conclude that the influence of aerosol cleanup (SSP2-4.5) has a larger influence on ΔP than do changes in circulation for both Equatorial Africa and SE Asia (Fig. 4 a, c). When aerosol emissions follow a regional rivalry framework (SSP3-7.0), the influence of aerosol radiative changes is of an equivalent magnitude to circulation changes in Equatorial Africa (where aerosol increases) and is smaller than the circulation influence in SE Asia, where aerosol remains almost constant (Fig. 4 b, d). Although circulation changes clearly influence regional precipitation trends over the 21st century, such changes are unlikely to exceed those driven by local cleanup efforts in regions with high loadings of absorbing aerosol. We conclude that aerosol cleanup (in SSP2-4.5, compared with SSP3-7.0) has a major influence on SW absorption, and will accelerate increases in precipitation in both regions examined.

5 Quantifying absorbing aerosol influences on precipitation

These atmospheric energy budget examinations provide compelling evidence that future choices in aerosol emissions will influence precipitation over the 21st century, both regionally and globally. Absorbing aerosol, via ΔSW, affects precipitation through the fast (i.e., temperature-independent) response (Allen & Ingram, 2002). In this section, we quantify the fast response associated with $\Delta AAOD$ using three different analysis methods.

The first and simplest method uses multiple linear regression to establish temperature-dependent and AAOD-dependent influences on ΔP (Fig. 5a). This regression explains 86% of the variance in global ΔP across all SSPs at 95% confidence. Using the coefficient for the $\Delta AAOD$ contribution, we estimate the aerosol-driven portion of ΔP (ΔP_{AAOD}) for each scenario (Fig. 5b).

The second method follows Allan et al. (2020), producing an independent estimate of the fast response that does not use $\Delta AAOD$. We estimate the temperature-dependent precipitation response (η) and the combined temperature-dependent and independent response (η_a) from Fig. 1b (see Section 3). The fast precipitation response for SSPs is the difference between these hydrologic sensitivities:

$$\Delta P_{fast} = \Delta T \left(\eta - \eta_a \right). \tag{6}$$

Table S2 shows η, η_a, and ΔP_{fast} global estimates by scenario. We expect η to be scenario independent since it is a model-specific quantity and all SSP simulations use the same set of CMIP6 models. Indeed, individual SSP η's are within uncertainties of each other. For consistency in our calculations, we use the scenario mean value for all SSPs, $\overline{\eta_{SSP}}$=2.02 ± 0.26 W m^{-2} K^{-1} (Table S2). This is within uncertainties of a multi-model mean estimate from abrupt 4xCO2 CMIP6 simulations, η=2.16 W m^{-2} K^{-1} (Pendergrass, 2020).

The fast response includes contributions from changes in absorbing aerosols as well as WMGHGs, most importantly ΔCO_2 and, to a lesser extent, ΔCH_4 and other WMGHG:

$$\Delta P_{fast} = \Delta P_{fast,AAOD} + \Delta P_{fast,CO2} + \Delta P_{fast,CH4} + \Delta P_{fast,other}. \tag{7}$$

To calculate $\Delta P_{fast,AAOD}$ for each scenario from Eq. 7, we use ΔP_{fast} estimates (Table S2) and assume $\Delta P_{fast,other}$ is negligible. We rely on Richardson et al. (2018)'s sensitivity studies to estimate fast precipitation responses for the two dominant WMGHGs (CO_2 and CH_4): a doubling of CO_2 has a -2.2 W m^{-2} response while a tripling of CH_4 has -0.5 W m^{-2} (see their Fig. 1). Assuming contributions of CO_2 and CH_4 to the fast response depend logarithmically on concentration (consistent with Andrews et al. (2010) and Laakso et al. (2020)), we construct the following equations for fast responses from

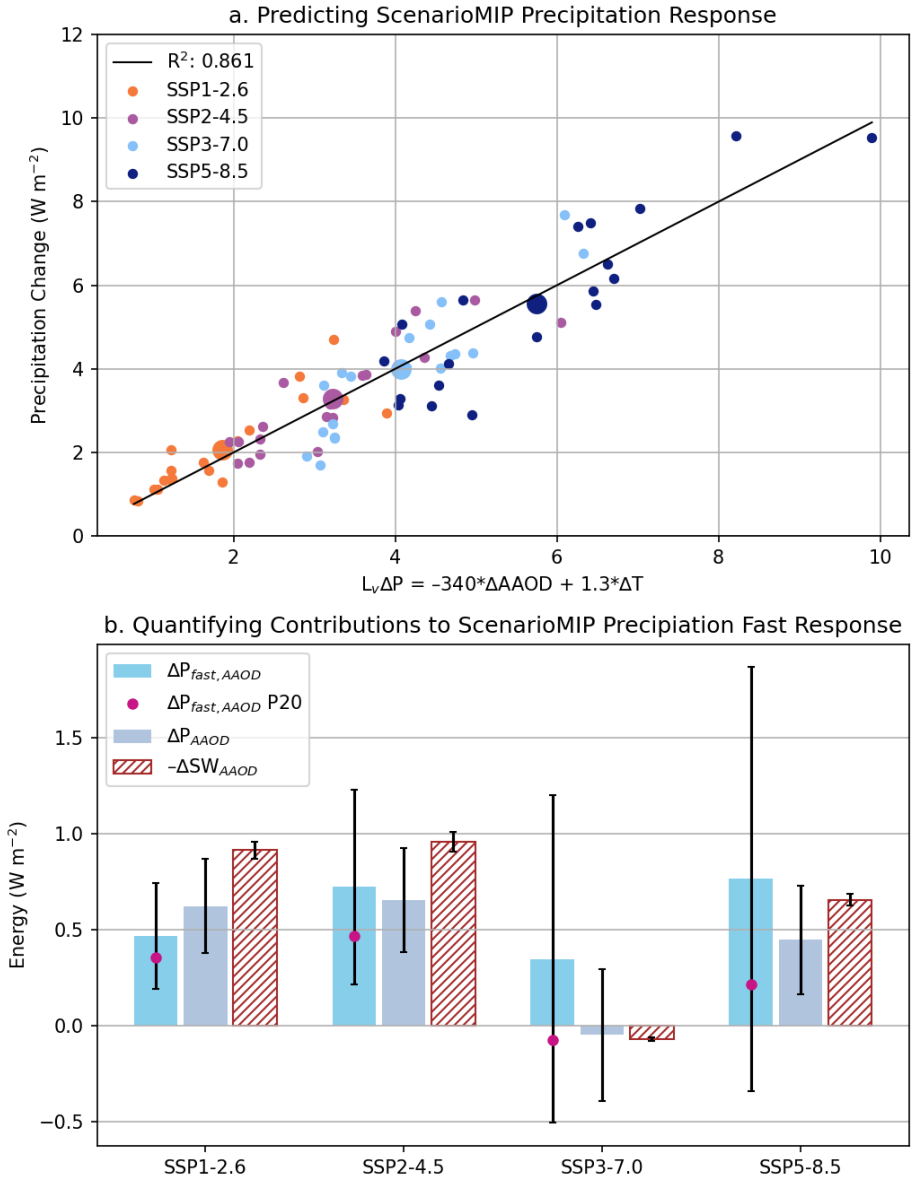

Figure 5. Quantifying the fast precipitation responses in ScenarioMIP simulations through various methods. (a) A multiple linear regression on $\Delta AAOD$ and ΔT for global ensemble members across all SSPs explains 86% of the variance at 95% confidence of the total precipitation response, ΔP. (b) Using the relationship in (a), we estimate the AAOD contribution, ΔP_{AAOD}, and contrast it with estimates of $\Delta P_{fast,AAOD}$, explained in the text, and ΔSW_{AAOD}. The $\Delta P_{fast,AAOD}$ P20 comparison (red circle) uses η=2.16 (Pendergrass, 2020) instead of 2.02 W m^{-2} K^{-1} (this study). All of these temperature-independent energy terms are significantly smaller for SSP3-7.0 than in the other SSPs, signifying the importance of $\Delta AAOD$ in determining ΔP. Bars represent multi-model mean and errors represent one SE instead of 2SE to account for large uncertainty in $\Delta P_{fast,AAOD}$ for SSP5-8.5.

arbitrary gas concentration changes:

$$\Delta P_{fastCO2} = -\left(\frac{2.2}{\ln 2}\right)\ln\left(\frac{[CO_2^f]}{[CO_2^i]}\right)$$
$$\Delta P_{fastCH4} = -\left(\frac{0.5}{\ln 3}\right)\ln\left(\frac{[CH_4^f]}{[CH_4^i]}\right) \quad (8)$$

Superscripts i and f in Eq. 8 indicate initial (2015-2025 mean) and final (2090-2100 mean) concentrations, respectively. Gas concentrations are from Meinshausen et al. (2020). These contributions to ΔP_{fast} and the final $\Delta P_{fast,AAOD}$ (Fig. 5b) are listed in Table S2 by scenario. We also include an estimate of $\Delta P_{fast,AAOD}$ in Fig. 5b using η from Pendergrass (2020) (P20) that falls within uncertainties, suggesting $\Delta P_{fast,AAOD}$ is not overly sensitive to our η determination.

The only other WMGHG that contributes significantly to the atmospheric energy budget is nitrous oxide (N_2O), but estimates of its impact on fast precipitation responses are not available in the literature. The TOA forcing from N_2O over the 21st century is estimated to be less than 0.3 W m^{-2} for all SSPs studied here (Meinshausen et al., 2020). Assuming the fast precipitation response from N_2O scales similarly with TOA forcing as for other WMGHG (CO_2 and CH_4), then $\Delta P_{fast,N2O}$ would range from -0.05 W m^{-2} in SSP1-2.6 to -0.13 W m^{-2} in SSP3-7.0. The small range and magnitude of these estimated responses, and the significant statistical uncertainties in the estimates of ΔP_{fast} (Table S2), justifies our choice to exclude the effects of N_2O from our estimates of $\Delta P_{fast,AAOD}$.

The third method relies on the idea that changes in atmospheric SW absorption from aerosol (ΔSW_{AAOD}) translate into precipitation changes in the absence of changes in the other energy budget terms (ΔSH, ΔLW, and ΔSW_{WVP}). Since the relative changes in these other terms are small across scenarios (Figs. 1, 2), ΔSW_{AAOD} is an approximate estimate of the global ΔP due to absorbing aerosol changes (Fig. 5b).

Despite the large uncertainty in the residual estimation of $\Delta P_{fast,AAOD}$, we find relatively good agreement across scenarios between $\Delta P_{fast,AAOD}$ and ΔP_{AAOD} determined from regressing ΔP against ΔT and $\Delta AAOD$ (Fig. 5b). All methods agree that SSP3-7.0 has a precipitation response to AAOD that is very small compared with other scenarios, consistent with little global aerosol clean up (Fig. 1a). The variation of precipitation response to $\Delta AAOD$ across scenarios is also consistent with our independent expectations from the atmospheric energy budget, as shown by reductions in shortwave absorption by aerosol ($\Delta SW_{AAOD} < 0$) over the 21st century in all scenarios except SSP3-7.0 (Fig. 5b).

The general agreement between the three approaches to estimating absorbing aerosol influences on 21st century precipitation changes from ScenarioMIP simulations provides confidence that aerosol cleanup policies can lead to global precipitation rate increases in excess of 0.5 W m^{-2} ($\approx$0.6% increases on present day rates). Although this is relatively modest when compared with precipitation increases projected for the higher radiative forcings (e.g., $\sim$6% in SSP5-8.5 by the end of the century), if policies for CO_2 mitigation are more aggressive, then absorbing aerosol cleanup will constitute a much stronger contribution to precipitation increases in the coming century.

6 Summary

We use data from the ScenarioMIP suite of CMIP6 model simulations to explore the influence of absorbing aerosols on precipitation changes for four scenarios over the 21st century. Atmospheric energy and water budgets are used to examine influences of different controls on precipitation, both globally and regionally, between 2015-2025 and 2090-2100. As expected, precipitation increases of 2-3% K^{-1} are typical because atmo-

spheric radiative cooling is unable to keep pace with water vapor increases, which follow Clausius-Clapeyron. Precipitation increases are greater for scenarios with strong 21st century aerosol cleanup. We use a regression approach to isolate the temperature-independent effects of absorbing aerosol on the shortwave energy budget from the temperature-dependent effects of water vapor. We show that the apparent global hydrologic sensitivity is 40% stronger in SSP2-4.5 (aerosol clean up) than in SSP3-7.0 (no clean up), and this can be explained primarily by reduced 21st century SW absorption by aerosol in the former scenario.

This absorbing aerosol influence is found to significantly affect precipitation at the regional scale. Two regions are examined, Equatorial Africa (15°S-15°N, 30°W-30°E) and Southeast Asia (0-45°N, 60-130°E), which both experience aerosol cleanup during SSP2-4.5 but have differing aerosol emissions in SSP3-7.0. The influence of aerosol cleanup on precipitation via atmospheric shortwave absorption is estimated to be larger than the impacts of circulation changes in both regions.

The influence of absorbing aerosols on precipitation through the fast, temperature-independent response is quantified for all ScenarioMIP projections using both the hydrologic sensitivity and a multiple linear regression against ΔT and $\Delta AAOD$. Estimates are consistent with atmospheric energy budget estimations of $AAOD$ influence, suggesting absorbing aerosol cleanup policies are likely to boost global precipitation responses by at least 0.5 W m^{-2} ($\approx$0.6% of the present-day global mean rate). For scenarios with aggressive greenhouse gas mitigation (lower forcing), the aerosol-driven increases in precipitation can significantly accelerate the increases expected from climate warming. This study highlights the importance of considering aerosol emissions in future policy decisions as those choices will have critical and long-lasting impacts on both global and regional precipitation and, as a result, water availability in the future.

Acknowledgments

We thank Angeline Pendergrass and Dargan Frierson for helpful discussions of this work. We also acknowledge the World Climate Research Programme and its Working Group on Coupled Modelling for coordinating CMIP6; the climate modeling groups involved for their simulations; the Earth System Grid Federation (ESGF) for archiving and facilitating data usage; and the multiple funding agencies who support CMIP and ESGF efforts. Research by ILM is supported by the NOAA Climate and Global Change Postdoctoral Fellowship Program, administered by UCAR's Cooperative Programs for the Advancement of Earth System Science (CPAESS) under award NA18NWS4620043B. MV was funded on indirect cost recovery support from grants to UW.

Data Availability: All CMIP6 ScenarioMIP simulations used in this study are available at https://esgf-node.llnl.gov/projects/cmip6/.

References

Allan, R. P., Barlow, M., Byrne, M. P., Cherchi, A., Douville, H., Fowler, H. J., ... Zolina, O. (2020). Advances in understanding large-scale responses of the water cycle to climate change [Journal Article]. *Ann N Y Acad Sci*, *1472*(1), 49-75. Retrieved from `https://www.ncbi.nlm.nih.gov/pubmed/32246848` doi: 10.1111/nyas.14337

Allan, R. P., Liu, C., Zahn, M., Lavers, D. A., Koukouvagias, E., & Bodas-Salcedo, A. (2014, May). Physically Consistent Responses of the Global Atmospheric Hydrological Cycle in Models and Observations. *Surveys in Geophysics*, *35*(3), 533–552. Retrieved 2021-08-24, from `https://doi.org/10.1007/s10712-012-9213-z` doi: 10.1007/s10712-012-9213-z

Allen, M. R., & Ingram, W. J. (2002). Constraints on future changes in climate and

the hydrologic cycle [Journal Article]. *Nature*, *419*(6903), 228-232. Retrieved from https://doi.org/10.1038/nature01092https://www.nature.com/articles/nature01092a.pdf doi: 10.1038/nature01092

Andrews, T., Forster, P. M., Boucher, O., Bellouin, N., & Jones, A. (2010). Precipitation, radiative forcing and global temperature change. *Geophysical Research Letters*, *37*(14). Retrieved 2020-09-04, from https://agupubs.onlinelibrary.wiley.com/doi/abs/10.1029/2010GL043991 (_eprint: https://agupubs.onlinelibrary.wiley.com/doi/pdf/10.1029/2010GL043991) doi: 10.1029/2010GL043991

Dagan, G., & Stier, P. (2020). Constraint on precipitation response to climate change by combination of atmospheric energy and water budgets [Journal Article]. *npj Climate and Atmospheric Science*, *3*(1). doi: 10.1038/s41612-020-00137-8

Dagan, G., Stier, P., & Watson-Parris, D. (2019a). Analysis of the atmospheric water budget for elucidating the spatial scale of precipitation changes under climate change [Journal Article]. *Geophys Res Lett*, *46*(17-18), 10504-10511. Retrieved from https://www.ncbi.nlm.nih.gov/pubmed/31762521 doi: 10.1029/2019GL084173

Dagan, G., Stier, P., & Watson-Parris, D. (2019b). Contrasting response of precipitation to aerosol perturbation in the tropics and extratropics explained by energy budget considerations [Journal Article]. *Geophys Res Lett*, *46*(13), 7828-7837. Retrieved from https://www.ncbi.nlm.nih.gov/pubmed/31598021 doi: 10.1029/2019GL083479

Dagan, G., Stier, P., & Watson-Parris, D. (2021). An Energetic View on the Geographical Dependence of the Fast Aerosol Radiative Effects on Precipitation. *Journal of Geophysical Research: Atmospheres*, *126*(9), e2020JD033045. Retrieved 2021-05-28, from https://agupubs.onlinelibrary.wiley.com/doi/abs/10.1029/2020JD033045 (_eprint: https://agupubs.onlinelibrary.wiley.com/doi/pdf/10.1029/2020JD033045) doi: https://doi.org/10.1029/2020JD033045

DeAngelis, A. M., Qu, X., Zelinka, M. D., & Hall, A. (2015, December). An observational radiative constraint on hydrologic cycle intensification. *Nature*, *528*(7581), 249–253. Retrieved 2020-05-22, from https://www.nature.com/articles/nature15770 (Number: 7581 Publisher: Nature Publishing Group) doi: 10.1038/nature15770

Eyring, V., Bony, S., Meehl, G. A., Senior, C. A., Stevens, B., Stouffer, R. J., & Taylor, K. E. (2016, May). Overview of the Coupled Model Intercomparison Project Phase 6 (CMIP6) experimental design and organization. *Geoscientific Model Development*, *9*(5), 1937–1958. Retrieved 2019-11-15, from https://www.geosci-model-dev.net/9/1937/2016/ doi: 10.5194/gmd-9-1937-2016

Held, I. M., & Soden, B. J. (2006). Robust responses of the hydrological cycle to global warming [Journal Article]. *Journal of Climate*, *19*(21), 5686-5699. Retrieved from https://journals.ametsoc.org/view/journals/clim/19/21/jcli3990.1.xml doi: 10.1175/jcli3990.1

Laakso, A., Snyder, P. K., Liess, S., Partanen, A.-I., & Millet, D. B. (2020, May). Differing precipitation response between solar radiation management and carbon dioxide removal due to fast and slow components. *Earth System Dynamics*, *11*(2), 415–434. Retrieved 2021-12-22, from https://esd.copernicus.org/articles/11/415/2020/ (Publisher: Copernicus GmbH) doi: 10.5194/esd-11-415-2020

Lacis, A. A., & Hansen, J. (1974, January). A Parameterization for the Absorption of Solar Radiation in the Earth's Atmosphere. *Journal of the Atmospheric Sciences*, *31*(1), 118–133. Retrieved 2021-12-22, from https://journals.ametsoc.org/view/journals/atsc/31/1/

1520-0469_1974_031_0118_apftao_2_0_co_2.xml (Publisher: American Meteorological Society Section: Journal of the Atmospheric Sciences) doi: 10.1175/1520-0469(1974)031⟨0118:APFTAO⟩2.0.CO;2

Lund, M. T., Myhre, G., & Samset, B. H. (2019, November). Anthropogenic aerosol forcing under the Shared Socioeconomic Pathways. *Atmospheric Chemistry and Physics*, *19*(22), 13827–13839. Retrieved 2020-05-22, from https://www.atmos-chem-phys.net/19/13827/2019/ (Publisher: Copernicus GmbH) doi: https://doi.org/10.5194/acp-19-13827-2019

Meinshausen, M., Nicholls, Z. R. J., Lewis, J., Gidden, M. J., Vogel, E., Freund, M., ... Wang, R. H. J. (2020). The shared socio-economic pathway (ssp) greenhouse gas concentrations and their extensions to 2500 [Journal Article]. *Geoscientific Model Development*, *13*(8), 3571-3605. doi: 10.5194/gmd-13-3571-2020

Myhre, G., Samset, B. H., Schulz, M., Balkanski, Y., Bauer, S., Berntsen, T. K., ... Zhou, C. (2013). Radiative forcing of the direct aerosol effect from aerocom phase ii simulations [Journal Article]. *Atmospheric Chemistry and Physics*, *13*(4), 1853-1877. doi: 10.5194/acp-13-1853-2013

Neill, B. C., Tebaldi, C., van Vuuren, D. P., Eyring, V., Friedlingstein, P., Hurtt, G., ... Sanderson, B. M. (2016). The scenario model intercomparison project (scenariomip) for cmip6 [Journal Article]. *Geoscientific Model Development*, *9*(9), 3461-3482. doi: 10.5194/gmd-9-3461-2016

Pendergrass, A. G. (2020). The global-mean precipitation response to co 2 -induced warming in cmip6 models [Journal Article]. *Geophysical Research Letters*, *47*(17). doi: 10.1029/2020gl089964

Pendergrass, A. G., & Hartmann, D. L. (2012). Global-mean precipitation and black carbon in AR4 simulations. *Geophysical Research Letters*, *39*(1). Retrieved 2020-05-22, from https://agupubs.onlinelibrary.wiley.com/doi/abs/10.1029/2011GL050067 (_eprint: https://agupubs.onlinelibrary.wiley.com/doi/pdf/10.1029/2011GL050067) doi: 10.1029/2011GL050067

Pendergrass, A. G., & Hartmann, D. L. (2014). The atmospheric energy constraint on global-mean precipitation change [Journal Article]. *Journal of Climate*, *27*(2), 757-768. doi: 10.1175/jcli-d-13-00163.1

Riahi, K., van Vuuren, D. P., Kriegler, E., Edmonds, J., O'Neill, B. C., Fujimori, S., ... Tavoni, M. (2017). The shared socioeconomic pathways and their energy, land use, and greenhouse gas emissions implications: An overview [Journal Article]. *Global Environmental Change*, *42*, 153-168. doi: 10.1016/j.gloenvcha.2016.05.009

Richardson, T. B., Forster, P. M., Andrews, T., Boucher, O., Faluvegi, G., Fläschner, D., ... Voulgarakis, A. (2018). Drivers of precipitation change: An energetic understanding [Journal Article]. *Journal of Climate*, *31*(23), 9641-9657. doi: 10.1175/jcli-d-17-0240.1

Samset, B. H., Myhre, G., Forster, P. M., Hodnebrog, , Andrews, T., Boucher, O., ... Voulgarakis, A. (2018, January). Weak hydrological sensitivity to temperature change over land, independent of climate forcing. *npj Climate and Atmospheric Science*, *1*(1), 1–8. Retrieved 2021-07-16, from https://www.nature.com/articles/s41612-017-0005-5 (Bandiera_abtest: a Cc_license_type: cc_by Cg_type: Nature Research Journals Number: 1 Primary_atype: Research Publisher: Nature Publishing Group Subject_term: Climate and Earth system modelling;Projection and prediction Subject_term_id: climate-and-earth-system-modelling;projection-and-prediction) doi: 10.1038/s41612-017-0005-5

Samset, B. H., Myhre, G., Forster, P. M., Hodnebrog, , Andrews, T., Faluvegi, G., ... Voulgarakis, A. (2016). Fast and slow precipitation responses to individual climate forcers: A pdrmip multimodel study [Journal Article]. *Geophysical*

Research Letters, *43*(6), 2782-2791. doi: 10.1002/2016gl068064

Turnock, S. T., Allen, R. J., Andrews, M., Bauer, S. E., Deushi, M., Emmons, L., ... Zhang, J. (2020, November). Historical and future changes in air pollutants from CMIP6 models. *Atmospheric Chemistry and Physics*, *20*(23), 14547–14579. Retrieved 2021-11-16, from `https://acp.copernicus.org/articles/20/14547/2020/` (Publisher: Copernicus GmbH) doi: 10.5194/acp-20-14547-2020